SNR and CNR Performance Comparison in Dixon- vs. Subtraction-type Contrast Enhanced MR Angiography

Eric G. Stinson[1], Joshua D. Trzasko[1], and Stephen J. Riederer[1]
[1]*Mayo Clinic, Rochester, Minnesota, United States*

Target Audience: ISMRM members with interest in emerging contrast-enhanced MR angiography techniques.

Purpose: Contrast-enhanced MR angiography (CE-MRA) typically emphasizes contrast-enhanced luminal signal by suppressing non-vascular signal. Subtraction of a pre-contrast reference image is generally performed, necessitating a separate acquisition that is spatially registered with the contrast-filled image. In addition to the extra scan time required for the reference, the process is also prone to subtraction artifact in some anatomic regions (abdomen, thorax) due to motion. In gradient-echo (GRE)-based CE-MRA, it is the high lipid signal that typically obscures the contrast-enhanced vascular signal. Consequently, instead of a pre-contrast reference, some other means of fat suppression can be used. In the excitation process, inversion recovery preparation or selective suppression [1-3] can be used, but can be limited due to reduced signal-to-noise ratio (SNR) or inefficient fat suppression due to off-resonance effects. Recently, fat-suppressed CE-MRA utilizing the water-only image from a generalized dual-echo Dixon-type method [4] has been reported to actually increase the SNR and contrast-to-noise ratio (CNR) above that of pre-contrast reference-subtracted CE-MRA [5]. That is, such methods can potentially provide the benefits of fat suppression, eliminate the pre-contrast reference acquisition, and provide an SNR improvement. The purpose of this work is to investigate in detail the behavior of the CNR and SNR of Dixon methods compared to subtraction CE-MRA with a theoretical analysis and evaluation in numerical and physical phantoms.

Methods: *Theory:* SNR and CNR ratios of SNR_{Dixon}/SNR_{sub} and CNR_{Dixon}/CNR_{sub} were derived and used to evaluate SNR or CNR differences at a number of contrast agent concentrations. Beginning with the forward models for a subtraction-type (1) and a Dixon-type reconstruction (2), SNR of the reconstructed images was derived according to (3) where H is the pseudo-inverse of A. Here, the specific example of the dual-echo case is used, but a general expression for any number of echoes has been derived. Making further signal assumptions, we obtain the SNR and CNR ratio expressions in equations (4) and (5). Note that θ_j is dependent on the chemical shift of fat, Δf, and the chosen echo times, TE_j, and that f_{Dixon} and f_{sub} can be calculated using the signal equation for spoiled gradient echo acquisition, which depends on flip angle, repetition time TR, and TE.

$$g_{\text{sub}} = A_{sub} f_{\text{sub}} + n_{\text{sub}} \tag{1}$$

$$\begin{bmatrix} g_1 \\ g_2 \end{bmatrix} = A_{Dixon} \begin{bmatrix} f_{water} \\ f_{lipid} \end{bmatrix} + \begin{bmatrix} n_1 \\ n_2 \end{bmatrix}$$

$$A_{Dixon} = \begin{bmatrix} e^{i\varphi_1} & 0 \\ 0 & e^{i\varphi_2} \end{bmatrix} \begin{bmatrix} 1 & e^{i\theta_1} \\ 1 & e^{i\theta_2} \end{bmatrix} \quad \begin{matrix} \varphi_j = \gamma \Delta B_0 (TE_j) \\ \theta_j = 2\pi \Delta f (TE_j) \end{matrix} \tag{2}$$

$$SNR = \frac{|HAf|}{\sqrt{\mathbb{E}[Hnn^H H^H]_{i,i}}} = \frac{|f|}{\sqrt{[H\Psi H^H]_{i,i}}} \tag{3}$$

$$\frac{SNR_{Dixon}}{SNR_{sub}} = \frac{|f_{\text{CE}}|}{|f_{\text{CE}} - f_{water}|} \sqrt{2}\sqrt{1 - \cos(\theta_2 - \theta_1)} \tag{4}$$

$$\frac{CNR_{Dixon}}{CNR_{sub}} = \sqrt{2}\sqrt{1 - \cos(\theta_2 - \theta_1)} \tag{5}$$

Numerical Phantom: Experiments were performed in MATLAB (R2012a, The Mathworks, Natick, MA) to test the accuracy of the derived ratios. Differing amounts of complex noise were added to a noise-free phantom created with the Fat-Water Toolbox [6] and reconstructed by direct matrix inversion. Field inhomogeneities and T_2^* effects were not included. The mean of the vessel and background signal and standard deviation of the noise were measured and used to calculate SNR and CNR ratios. *Physical Phantom:* Experiments were performed with an anthropomorphic fat-water phantom having an outer layer of vegetable shortening surrounding a bovine gelatin center to simulate an abdomen with subcutaneous fat. Six vials of bovine gelatin with differing concentrations of Gadolinium were inserted into a void in the center of the phantom to simulate an enhancing abdominal aorta. The physical phantom was scanned at 3 Tesla (General Electric, Waukesha, WI) with the following scan parameters: TE1/TE2/TR=2.3/3.5/6.5msec, α=18^0, BW=±62.5kHz, FOV=22cm, Slice thickness=2mm, Matrix: 224x224x30. For these echo times, $\theta_2 - \theta_1$ = 193^0. Images were fully sampled with a birdcage head coil. Region-of-interest based measurements were compared to the derived SNR and CNR ratios with signal calculated from scan parameters and phantom properties. Dixon images were formed using a generalized dual-echo reconstruction [4].

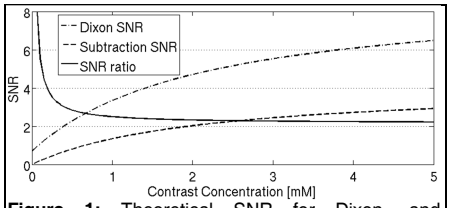

Figure 1: Theoretical SNR for Dixon- and subtraction-type CE-MRA, compared with the ratio of the two.

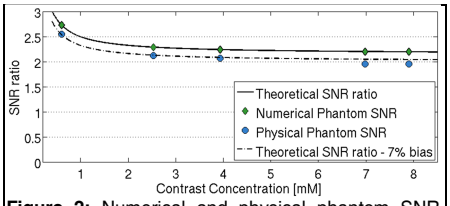

Figure 2: Numerical and physical phantom SNR ratios compared to theoretical values calculated from phantom properties and sequence parameters.

Results: *Theory:* Figure 1 shows a plot of theoretical SNR for Dixon-based and conventional subtraction CE-MRA as a function of the concentration of contrast material in the blood. The non-linear behavior of each is due to the non-linear dependence of the GRE signal on the contrast-enhanced T1 of the blood. The relative SNR improvement for the Dixon approach is due to (i) the intrinsic averaging effect of the two echoes of the Dixon processing, and (ii) the Dixon signal, f_{CE}, is always larger than the subtraction MRA signal, $f_{\text{CE}} - f_{water}$. *Numerical Phantom:* Results are shown in Figure 2. SNR and CNR (not shown) ratio values in the numerical phantom match theory very closely at all noise levels, although some variation occurs at high noise values. *Physical Phantom:* Results from the experiments with the physical phantom are also shown in Figure 2. Other than a bias of approximately 7%, the empirical values track the theoretical values well.

Discussion: CNR shows an improvement of approximately a factor of 2 at the chosen echo times. Interestingly, the CNR is constant over all contrast concentrations, as expected from the signal approximations. In phantoms, this approximation held fairly well, as the same material (undoped bovine gelatin) was used to simulate unenhanced blood and static tissue. *In vivo*, these signal assumptions may not hold when the surrounding tissue signal differs from that of unenhanced blood. Unlike CNR, the SNR ratio retains a dependence on signal, giving Dixon MRA a larger SNR advantage at lower contrast concentrations. This can be understood by examining the signal dependent portion of the SNR ratio: $S_{SNR} = |f_{\text{CE}}|/|f_{\text{CE}} - f_{water}|$. When $f_{\text{CE}} \gg f_{water}$, S_{SNR} reduces to unity; but at lower contrast doses, f_{CE} approaches f_{water} and S_{SNR} increases drastically. Indeed, when we examine the case where $f_{\text{CE}} = f_{water}$, we see that Dixon imaging has an infinite SNR advantage because the subtracted signal within the vessel is zero. In the physical phantom, we recognize the trend that theory predicts, but observe a bias of about 7%. This bias could be due to one or more of the elements not accounted for in our model, including T_2^* effects, incomplete spoiling, or B1 inhomogeneity. SNR and CNR are dependent on the difference in water-fat phase between the two echo times; however, for 164^0 < $(\theta_2 - \theta_1)$ < 196^0, improvement is at least 99% of the maximum possible improvement.

Conclusion: A theoretical and experimental comparison of SNR and CNR in Dixon CE-MRA and subtraction CE-MRA has been presented. Dixon CE-MRA shows a signal dependent SNR advantage of a factor of 2 or greater over subtraction CE-MRA and retains a constant CNR advantage of a factor of about 2 for appropriately chosen TEs. The advantage of Dixon-type CE-MRA is especially prominent at low contrast doses, where the subtracted signal within the vessel nears zero and the Dixon signal is only reduced according to the GRE signal equation. These results suggest that Dixon-type CE-MRA may be of particular use in situations where low contrast dose is desired.

References: [1] Bydder GM. JCAT;9:1084 (1985). [2] Haase A. Phys Med Biol;30:341 (1985). [3] Meyer CH. MRM;15:287 (1990). [4] Eggers H. MRM;65:96 (2011). [5] Leiner T. ISMRM 2011 - Melbourne, AUS. #0525 [6] Fat-Water Toolkit: http://ismrm.org/workshops/FatWater12/data.htm